24th COBEM - 2017

24th ABCM International Congress of Mechanical Engineering
December 3-8, 2017, Curitiba, PR, Brazil

COBEM-2017-2701
MODELLING AND CONTROLLING OF AN ELECTRIC POWERED WHEELCHAIR USING THE CONTROL LYAPUNOV FUNCTION

André Antunes Jorge
Luis Alberto M. Riascos
Engineering Center, Modelling and Applied Social Sciences, Federal University of ABC, Santo Andre, Sao Paulo, Brazil
e-mails: andre.anjorge@gmail.com; luis.riascos@ufabc.edu.br

Abstract. *There are several research about adaptabilities on wheelchairs moving through urban spaces considering obstacles, allowing disabled people to live and interact with society. It estimated that 110 milion people of the world's population have got significant difficulties in functioning. Demanding the development of better handicap equipments, this paper presents a method to control an Electric Powered Wheelchair (EPW), applying a safe driving closed-loop modelling, which controls the torque of the gearmotors. Firstly, a reliable mathematical model for an EPW, divided in kinematic and dynamic models, will be presented, through the use of the Lagrangian formalism. Second, knowing the propulsion and rotation velocities, the torque control applied on the drive wheels gearmotors was proposed, since the torque gives smooth and precise driving on the ground. Then, the control Lyapunov function (CLF) technique is presented to obtain a control law for controlling the angular velocity of the drive wheels, and consequently, it will control the EPW motion on a flat or inclined surface, as desired by the user. The EPW mathematical model was implemented in MATLAB®/Simulink, where a graphical user interface (GUI) was developed to intermediate the numerical simulations. Thus, the graphical results will be presented and discussed, showing the CLF technique converges for the desired result.*

Keywords: *System modelling, motion control, Electric Powered Wheelchair (EPW), torque, linear and angular velocities, control Lyapunov function (CLF).*

1. INTRODUCTION

According to World Health Organization (WHO), more than one billion people are estimated to live with some form of disability, or about 15% of the world's population. The World Health Survey (WHS) also estimates that 110 million people (15 years and older), or about 2.2% of the world's population, have very significant difficulties in functioning (World Health Organization, 2011). Thus, Electric Powered Wheelchairs (EPWs) provide functional mobility for people with motor disability. Over the years, great advances have been made in the design of EPWs (Riascos, 2015), though the control algorithms for these wheelchairs have improved comparatively little since the early 1980. Driving an EPW could become safer and more effective in a broader array of environments for more people with the application of advanced control systems (Ummat and Kirby, 1994; Cooper, 1999).

The aim of this paper is to provide a mathematical model of an EPW that can be controlled on a flat or inclined surface, based on controlling the torque applied on the drive wheels, since the torque gives smooth and precise driving on the ground (Park *et al.*, 2014). The applied controlling technique was the control Lyapunov function (CLF), in order to evaluate their behavior in an EPW. Lyapunov functions are a powerful tool for establishing stability properties of dynamical systems, such as Global Asymptotic Stability (GAS). The existence of a Lyapunov function is guaranteed by conversing Lyapunov theorems under the assumption that the system is GAS. Therefore, a continuous closed-loop Lyapunov function can be constructed by combining the function that defines the system of a EPW with a function that characterizes the Lyapunov function. Since the Lyapunov function is continuous, the closed-loop asymptotic stability has robustness (Geiselhart *et al.*, 2002).

2. DEVELOPMENT OF A 3D MATHEMATICAL MODEL FOR AN ELECTRIC POWERED WHEELCHAIR

2.1 Kinematic model of an Electric Powered Wheelchair

The free body diagram of an EPW on a flat and inclined surface (Toudjeu *et al.*, 2012; Onyango *et al.*, 2009, 2016; Coelho, 2001; Coelho and Urbano, 2003) is shown in Figure 1 (a) and (b), respectively.

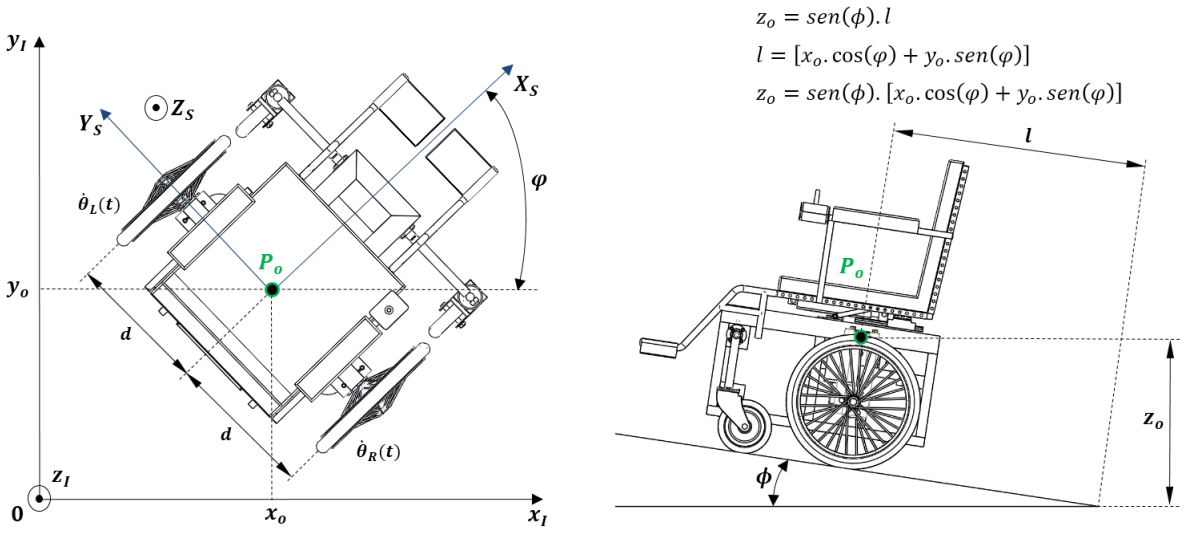

(a) (b)

Figure 1. Free body diagram of an EPW (a) on a flat surface, (b) on an inclined surface.

From the constraints generated by the types of wheels, the kinematic model of an EPW that moves on a flat and inclined surface can be expressed by Eq. (1) (Siegwart and Nourbakhsh, 2004):

$$\begin{cases} \dot{x}_0 = \dfrac{r}{2}cos(\varphi)cos(\phi)(\dot{\theta}_R + \dot{\theta}_L) \\ \dot{y}_0 = \dfrac{r}{2}sen(\varphi)cos(\phi)(\dot{\theta}_R + \dot{\theta}_L) \\ \dot{z}_0 = sen(\phi)\left[\dfrac{r}{2}(\dot{\theta}_R + \dot{\theta}_L) + \dot{\varphi}(y_0 cos(\varphi) - x_0 sen(\varphi))\right] \\ \dot{\varphi} = \dfrac{r}{2d}(\dot{\theta}_R - \dot{\theta}_L) \end{cases} , \tag{1}$$

where $\dot{x}_0$, $\dot{y}_0$ and $\dot{z}_0$ are linear velocities of, x, y and z axes, $\dot{\theta}_L$ and $\dot{\theta}_R$ are angular velocities of the left and right drive wheels, respectively, φ is the moving direction (orientation), ϕ is the slope angle of the ground (ramp), l is the linear displacement of the EPW on xy-plane, z_0 is the height of the EPW from the ground; r is the radius of the wheels; $2d$ is the distance between the drive wheels.

If the EPW moves on a flat surface, the value corresponding to the z axis does not vary.

2.2 Dynamic model of an Electric Powered Wheelchair

Some considerations are important for the model of an EPW. First of all, the EPW was considered as a rigid body, where it has two rear drive wheels and two front passive wheels (type castor). Each of the rear wheels is independently driven by a DC motor. Second, the center of mass is coincident with the center between the drive wheels, according to the point P_0 indicated in the Figure 1. Third, the angular velocity or rotation (orientation) of the EPW is defined as the difference between angular velocities of the right and left drive wheels. Fourth, two identical DC motors were considered to be used. The position of the EPW in the inertial frame (*x, y, z*) is specified completely by the generalized coordinates, $q = [x_0, y_0, z_0, \varphi, \theta_R, \theta_L]^T$, where x_0, y_0 and z_0 are the coordinates of the EPW center of mass.

The kinetic $T(q, \dot{q})$ and potencial $U(q)$ energies of the EPW are given by Eq. (2) and (3) (Bloch *et al.*, 2003):

$$T(q, \dot{q}) = \frac{1}{2}m(\dot{x_0}^2 + \dot{y_0}^2 + \dot{z_0}^2) + \frac{1}{2}I\dot{\varphi}^2 + \frac{1}{2}I_w(\dot{\theta_R}^2 + \dot{\theta_L}^2) , \tag{2}$$

$$U(q) = mgz_0 \rightarrow U(q) = mgsen(\phi)[x_0 cos(\varphi) + y_0 sen(\varphi)] , \tag{3}$$

where m is the EPW total mass, considering the person mass, and $I = 2m_w d^2 cos^2(\phi) + 2I_m + I_c + I_p$, being that m_w is the wheel mass, I_m is the wheel inertia on the z axis, I_c is the chassis inertia on the z axis, I_p is the user inertia on the z axis and I_w is the wheel inertia on the x axis (Bloch *et al.*, 2003; Coelho, 2001; Coelho and Urbano, 2003).

By subtracting the potencial energy from the kinetic energy, the Lagrange equation was obtained, according to Eq. (4) (Bloch *et al.*, 2003; Coelho, 2001; Coelho and Urbano, 2003; Onyango *et al.*, 2016):

$$\mathscr{L}(q,\dot{q}) = T(q,\dot{q}) - U(q) \rightarrow$$

$$\mathscr{L}(q,\dot{q}) = \frac{1}{2}m({\dot{x}_0}^2 + {\dot{y}_0}^2 + {\dot{z}_0}^2) + \frac{1}{2}I\dot{\varphi}^2 + \frac{1}{2}I_w({\dot{\theta}_R}^2 + {\dot{\theta}_L}^2) - mgsen(\phi)\big(x_0 cos(\varphi) + y_0 sen(\varphi)\big) \ . \tag{4}$$

The Lagrangian formalism, according to Eq. (5) (Bloch *et al.*, 2003), may be applied to derive the general set of differential equations that describes the time evolution of the EPW limited by nonholonomic kinematic constraints. In other words, it was found the dynamic equations for the EPW.

$$\frac{d}{dt}\left(\frac{\partial \mathscr{L}}{\partial \dot{q}_i}\right) - \frac{\partial \mathscr{L}}{\partial q_i} = F_i \ . \tag{5}$$

The general expression of a nonholonomic EPW with n–dimensional configuration space and generalised coordinates q subjected to a constraints may be described by (Onyango *et al.*, 2016):

$$M(q)\ddot{q} + C(q,\dot{q})\dot{q} + G(q) = B(q)\tau - F_R(q,\dot{q}) + A^T(q)\lambda \ , \tag{6}$$

where $M(q) \in R^{n\times n}$ is the inertia matrix and it is symmetric positive defined, $C(q,\dot{q}) \in R^{n\times n}$ is the matrix of corolis and centripetal forces, $G(q) \in R^{n\times 1}$ is a vector of gravitational forces, $B(q) \in R^{n\times r}$ is the input transformation matrix known as function of fixed geometry of a system, $\tau \in R^{n\times 1}$ is the input vector of torques and forces, $A(q) \in R^{a\times n}$ is the matrix related to nonholonomic constraints, λ is the vector of Lagrange multipliers, $F_R(q,\dot{q}) = F_c(q) + F_v(\dot{q}) = F_c(q) + \mu_v\dot{q}$, being that $F_c(q) \in R^{n\times 1}$ is the vector of Coulomb friction force, $F_v(\dot{q}) \in R^{n\times 1}$ is the vector of the viscous friction force and μ_v is the coefficient of viscous friction.

The independent and non integrable kinematic constraints may be expressed as (Coelho, 2001; Coelho and Urbano, 2003; Onyango *et al.*, 2009, 2016; Toudjeu *et al.*, 2012):

$$A(q)\dot{q} = 0 \ . \tag{7}$$

Considering $S(q) \in R^{n\times r}$ being a set of linearly independent and smooth vector field spanning the null space of $A(q)$, it is possible to state that (Onyango *et al.*, 2009; Coelho, 2001; Coelho and Urbano, 2003):

$$S(q).A(q) = S^T(q).A^T(q) = 0 \ . \tag{8}$$

The Eq.(**??**) may be transformed in the two equations following (Coelho, 2001; Coelho and Urbano, 2003):

$$\dot{q} = S(q).\vartheta(t) \ , \tag{9}$$

$$\overline{M}(q)\dot{\vartheta} + \overline{C}(q,\dot{q})\vartheta + \overline{G}(q) = \overline{B}(q)\tau - \overline{F_R}(q,\dot{q}) \ , \tag{10}$$

where the Eq.(9) represents the kinematic of the EPW. $S(q) \in R^{n\times r}$ generates the null space of $A(q)$ and it is a regular matrix. It is a Jacobian matrix that transforms the velocities ϑ described in the mobile coordinates system in velocities $\dot{q}$ defined in the cartesian coordinates system.

$$S(q) = \begin{bmatrix} \frac{r}{2}cos(\varphi)cos(\phi) & \frac{r}{2}cos(\varphi)cos(\phi) \\ \frac{r}{2}sen(\varphi)cos(\phi) & \frac{r}{2}sen(\varphi)cos(\phi) \\ \frac{r}{2}sen(\phi) & \frac{r}{2}sen(\phi) \\ \frac{r}{2d} & -\frac{r}{2d} \\ 1 & 0 \\ 0 & 1 \end{bmatrix}, \ \vartheta(t) = \begin{bmatrix} \dot{\theta_R} \\ \dot{\theta_L} \end{bmatrix}.$$

In turn, the Eq.(10) represents the EPW dynamic in a simplified form (Coelho, 2001; Coelho and Urbano, 2003), where:

$$\overline{M} = S^T M S \ , \tag{11}$$

$$\overline{C} = S^T(M\dot{S} + CS) \ , \tag{12}$$

$$\overline{G} = S^T G \ , \tag{13}$$

$$\overline{B} = S^T B \ , \tag{14}$$

$$\overline{F_R} = S^T F_c + S^T F_v \ . \tag{15}$$

By solving the Eq. (5), in relation to each generalized coordinate, the dynamic matrices were obtained:

$$M(q) = \begin{bmatrix} m & 0 & 0 & 0 & 0 & 0 \\ 0 & m & 0 & 0 & 0 & 0 \\ 0 & 0 & m & 0 & 0 & 0 \\ 0 & 0 & 0 & I & 0 & 0 \\ 0 & 0 & 0 & 0 & I_W & 0 \\ 0 & 0 & 0 & 0 & 0 & I_W \end{bmatrix}, C(q,\dot{q}) = 0 \ , G(q) = \begin{bmatrix} mgsen(\phi)cos(\varphi) \\ mgsen(\phi)sen(\varphi) \\ 0 \\ mgsen(\phi)[-x_o sen(\varphi) + y_o cos(\varphi)] \\ 0 \\ 0 \end{bmatrix},$$

$$B(q) = \begin{bmatrix} 0 & 0 \\ 0 & 0 \\ 0 & 0 \\ 0 & 0 \\ 1 & 0 \\ 0 & 1 \end{bmatrix}, \tau = \begin{bmatrix} \tau_R \\ \tau_L \end{bmatrix}, F_R = F_c(q) \begin{bmatrix} 0 \\ 0 \\ 0 \\ 0 \\ 1 \\ 1 \end{bmatrix} + \mu_v(\dot{q}) \begin{bmatrix} 0 \\ 0 \\ 0 \\ 0 \\ \dot{\theta}_R \\ \dot{\theta}_L \end{bmatrix}.$$

Then, by solving the equations from (11) to (15), the simplified dynamic matrices were obtained:

$$\overline{M}(q) = \begin{bmatrix} \frac{r^2}{4}\left(m + \frac{I}{d^2}\right) + I_w & \frac{r^2}{4}\left(m - \frac{I}{d^2}\right) \\ \frac{r^2}{4}\left(m - \frac{I}{d^2}\right) & \frac{r^2}{4}\left(m + \frac{I}{d^2}\right) + I_w \end{bmatrix}, \overline{C}(q,\dot{q}) = 0 \ ,$$

$$\overline{G}(q) = \begin{bmatrix} \frac{r}{2}mgsen(\phi)\left(cos(\phi) + \frac{y_0 cos(\varphi)}{d} - \frac{x_0 sen(\varphi)}{d}\right) \\ \frac{r}{2}mgsen(\phi)\left(cos(\phi) - \frac{y_0 cos(\varphi)}{d} + \frac{x_0 sen(\varphi)}{d}\right) \end{bmatrix}, \overline{B}(q) = \begin{bmatrix} 1 & 0 \\ 0 & 1 \end{bmatrix}, \tau = \begin{bmatrix} \tau_R \\ \tau_L \end{bmatrix},$$

$$\overline{F_R} = F_c \begin{bmatrix} 1 \\ 1 \end{bmatrix} + \mu_v \begin{bmatrix} \dot{\theta}_R \\ \dot{\theta}_L \end{bmatrix}.$$

Since the rolling friction (F_R) is nonlinear and dependent on many parameters, a reduced formulation that depends on the velocities $\dot{\theta}_R$ and $\dot{\theta}_L$ was considered. The reduced model is a combination of Coulomb and viscous friction, according to Eq. (16) (Fuss, 2009; Chua *et al.*, 2010):

$$F_R = F_c + F_v = \mu_c mg + \mu_v \dot{q} \ , \tag{16}$$

where μ_c is the coefficient of Coulomb friction.

The vector of Coulomb friction forces (F_c) and the vector of gravitional forces (G) will be removed from the Eq.(10) and they will be added to the load torque of the left and right wheels gearmotors. Since adding these forces to the load torque of the gearmotors, it also verify the impact (reduction of velocity) in the EPW dynamic. Thus, the dynamic equations that describe the movement of the left and right drive wheels of the EPW can be expressed as:

$$\tau_R = \left[\frac{r^2}{4}\left(m + \frac{I}{d^2}\right) + I_w\right]\ddot{\theta}_R + \left[\frac{r^2}{4}\left(m - \frac{I}{d^2}\right)\right]\ddot{\theta}_L + \mu_v \dot{\theta}_R \ , \tag{17}$$

$$\tau_L = \left[\frac{r^2}{4}\left(m - \frac{I}{d^2}\right)\right]\ddot{\theta}_R + \left[\frac{r^2}{4}\left(m + \frac{I}{d^2}\right) + I_w\right]\ddot{\theta}_L + \mu_v \dot{\theta}_L \ , \tag{18}$$

where τ_R and τ_L are torques of the right and left drive wheels, respectively.

2.3 Mathematical Model for Controlling an Electric Powered Wheelchair

By adding the torque equations, (17) and (18), and expressing them in function of wheels'acceleration, Eq. (19) was obtained (Park *et al.*, 2014):

$$(\tau_R + \tau_L) = \left[\frac{r^2}{2}m + I_w\right]\left(\ddot{\theta}_R + \ddot{\theta}_L\right) + \mu_v\left(\dot{\theta}_R + \dot{\theta}_L\right) \rightarrow$$

$$\left(\ddot{\theta}_R + \ddot{\theta}_L\right) = \frac{(\tau_R + \tau_L) - \mu_v\left(\dot{\theta}_R + \dot{\theta}_L\right)}{\frac{r^2}{2}m + I_w} \ . \tag{19}$$

By subtracting the torque equations , (17) and (18), and expressing them in function of wheels'acceleration, Eq. (20) was obtained (Park *et al.*, 2014):

$$(\tau_R - \tau_L) = \left[\frac{r^2 I}{2d^2} + I_w\right]\left(\ddot{\theta}_R - \ddot{\theta}_L\right) + \mu_v\left(\dot{\theta}_R - \dot{\theta}_L\right) \rightarrow$$

$$\left(\ddot{\theta}_R - \ddot{\theta}_L\right) = \frac{(\tau_R - \tau_L) - \mu_v\left(\dot{\theta}_R - \dot{\theta}_L\right)}{\frac{r^2 I}{2d^2} + I_w} \ . \tag{20}$$

It is assumed there is no slip between wheels and ground. Then, the propulsion or linear and rotation velocities of an EPW can be expressed by Eq. (21) (Park *et al.*, 2014):

$$\begin{cases} \nu = \dfrac{r}{2}\left(\dot{\theta}_R + \dot{\theta}_L\right) \\ \dot{\varphi} = \dfrac{r}{2d}\left(\dot{\theta}_R - \dot{\theta}_L\right) \end{cases} , \tag{21}$$

where, ν is the propulsion velocity and $\dot{\varphi}$ is the rotation velocity.

Hence, the time derivative of Eq. (21) can be represented as following (Park *et al.*, 2014):

$$\begin{cases} \dot{\nu} = \dfrac{r}{2}\left(\ddot{\theta}_R + \ddot{\theta}_L\right) \\ \ddot{\varphi} = \dfrac{r}{2d}\left(\ddot{\theta}_R - \ddot{\theta}_L\right) \end{cases} . \tag{22}$$

By substituting Eq. (18) and (19) in (22), the mathematical model to control an EPW can be expressed as (Park *et al.*, 2014):

$$\begin{cases} \dot{\nu} = \dfrac{r}{2}\left\{\dfrac{(\tau_R + \tau_L) - \mu_v\left(\frac{2\nu}{r}\right)}{\frac{r^2}{2}m + I_w}\right\} \\ \ddot{\varphi} = \dfrac{r}{2d}\left\{\dfrac{(\tau_R - \tau_L) - \mu_v\left(\frac{2d\dot{varphi}}{r}\right)}{\frac{r^2 I}{2d^2} + I_w}\right\} \end{cases} . \tag{23}$$

From the system of Eq. (23), a block diagram was developed in MATLAB®/Simulink for the numerical simulations, according to Figure 2.

2.4 Control Lyapunov function technique

The control Lyapunov function is used to test whether a system is stabilized by feedback. If for any state x there is a control $u(x,t)$, then the system can be routed to the null state when applying the control $u(x,t)$. In other words, the idea of this method is to verify if there is any type of energy measurement of the system states, where this energy decreases along a chosen path properly, then the system can approach a configuration of minimum energy (Sontag, 1990). Thus, to exist a Lyapunov function it is necessary to meet the following conditions of existence (Khalil, 2002):

- **1**st **Condition:** The function $V(x,t)$ must be continuous and positive defined throughout the domain, except in $x = 0$, where it must be null, as expressed in (24):

$$\begin{cases} x = 0, V(x,u) = 0 \\ \forall\ x \neq 0, \exists\ u\ \mid\ V(x,u) > 0 \end{cases}. \tag{24}$$

- **2**nd **Condition:** The derivative of the Lyapunov function, $\dot{V}(x,t)$, must be negative defined throughout the domain, except in $x = 0$, where it must be null, as expressed in (25):

$$\begin{cases} x = 0, \dot{V}(x,u) = 0 \\ \forall\ x \neq 0, \exists\ u\ \mid\ \dot{V}(x,u) < 0 \end{cases}. \tag{25}$$

The Lyapunov function used is a quadratic function, given by: $V_1(x,u) = \frac{1}{2}z_1^2$. Where z_1 represents the angular velocity error signal of each drive wheel.

Thus, by using the procedures of the CLF (Khalil, 2002), the control law (u), expressed in Eq. (26), was obtained:

$$u(t) = \frac{\left(\frac{B}{J} + \frac{k^2}{JR_a} - C_1\right)\omega(t) + \left(\frac{kL_a\frac{di_a}{dt}(t)}{JR_a} + \frac{T_L}{J}\right) + \dot{y}_{ref}(t) + C_1 y_{ref}(t)}{\frac{k}{JR_a}}, \tag{26}$$

where ω is the angular velocity (achieved velocity), L_a is the motor armature inductance, R_a is the motor armature resistance, k is the motor constant, J is the motor inertia, B is the motor viscous friction, i_a is the motor armature electrical current, T_L is the motor load torque, y_{ref} is the reference angular velocity (desired velocity), C_1 is a constant of project $(C_1 > 0)$ and u represents the motor input electrical voltage.

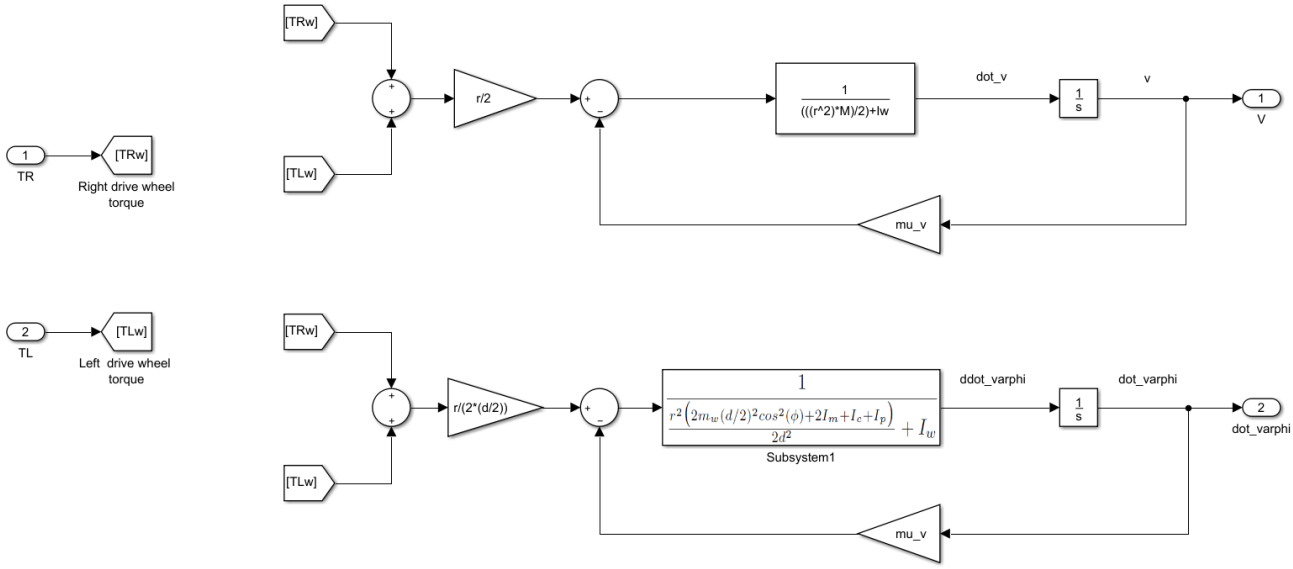

Figure 2. Block diagram of the EPW dynamic model.

2.5 Simulator for Controlling the Electric Powered Wheelchair Model

By using MATLAB®/Simulink, a graphical user interface (GUI) was created, in order to simulate the EPW model. It is worth mentioning this simulator can also simulate other types of EPW. However, the user must have all the requested parameters in the EPW Parameters panel, according to Figure 3.

Initially, the user enters the parameters or loads the default parameters. After that, it is necessery to select a position for the joystick, for example "North". The display "Motors Voltage" shows the voltage that will be applied on the right and left gearmotors. By pressing the chosen button of the joystick position, the voltage value applied to the gearmotors is varied. It is also necessary to enter the simulation time, in seconds, and the slope angle of the ground, in degrees. Then, the user must push the "Simulate" button and the EPW motion is presented in a specific window on a xy-plane. The user also can push different buttons of the joystick to move the EPW as desired, as well as choose a slope angle for the ground,

by pressing the ENTER key after entering the value. In addition, the user also can apply one or more disturbances on each gearmotor (right and left) with equal or different values of amplitude and time. When the simulation is completed or if the user pushes the "Stop" button, graphs of the electrical voltage and current, torque, desired and simulated angular velocities, and the error between these velocities over time for the right and left gearmotors will be shown. It will be also shown the graphs of the linear and rotation velocities, as well as the position and orientation of the EPW on 2D plane and 3D space.

3. RESULTS

Figure 3 shows the GUI of the EPW Simulator and the numerical simulation results for a angle of 4^o of the ground slope and with 40 seconds for the simulation time, from the parameters of an EPW, according to Table 1. It is important to mention the curves on the graphs represent the desired (reference) control, open-loop (MA) control and CLF.

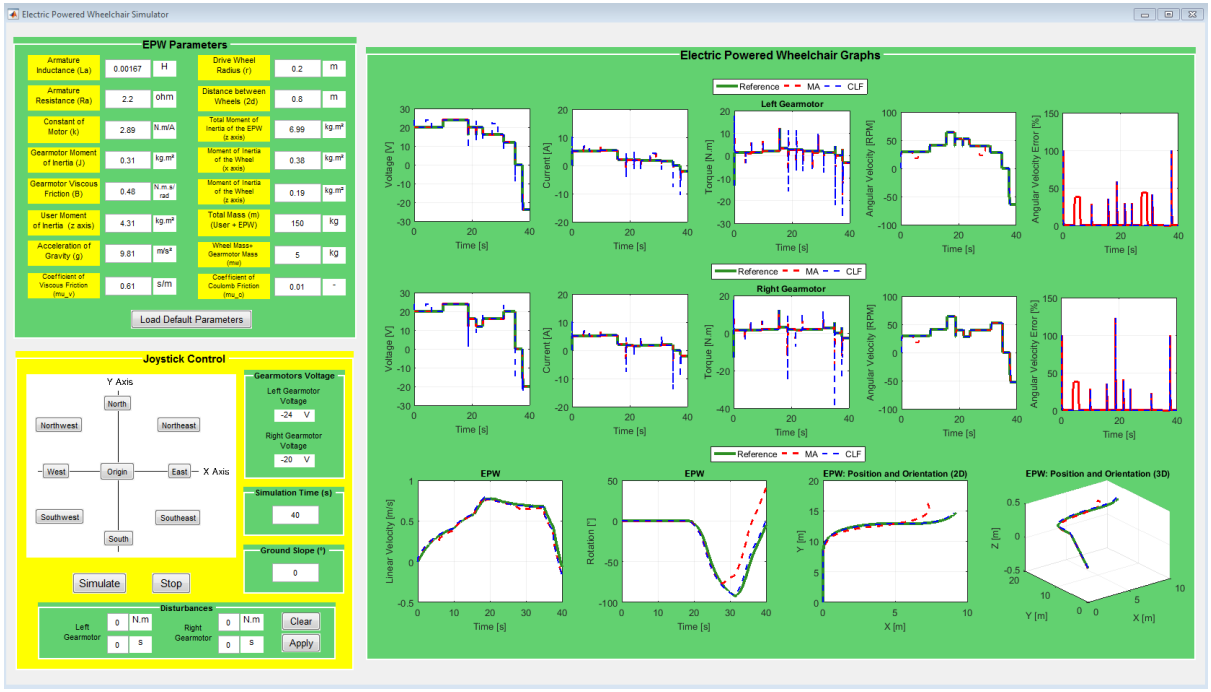

Figure 3. Electric Powered Wheelchair Simulator.

Table 1. Parameters of the EPW + User.

Armature Inductance (La)	1.67 mH
Armature Resistance (Ra)	2.2 Ω
Constant of Motor (k)	2.89 $N.m/A$
Inertia of Motor (J)	0.31 $kg.m^2$
Viscous Friction of Motor (B)	0.48 $N.m.s/rad$
Drive Wheel Radius (r)	0.20 m
Distance between Wheels ($2d$)	0.40 m
Total Mass (EPW = 70 kg + User = 80 kg) (m)	150.00 kg
Wheel Mass + Gearmotor Mass (m_w)	5.00 kg
Total Moment of Inertia (EPW) (I)	6.99 $kg.m^2$
Wheel Moment of Inertia (x axis) (I_w)	0.38 $kg.m^2$
Wheel Moment of Inertia (z axis) (I_m)	0.19 $kg.m^2$
User Moment of Inertia (z axis) (I_p)	4.31 $kg.m^2$
Acceleration of Gravity (g)	9.81 m/s^2
Coefficient of Coulomb friction (μ_c)	0.01
Coefficient of viscous friction (μ_v)	0.61 s/m
Constant of Project (C_1)	25.00

By plotting the graphs of the desired (reference), open-loop and CLF angular velocities and the error between the velocities over time for the left and right gearmotors, in a larger scale, as illustrated in Figures 4 and 5, it can be verified that the curves of the open-loop and CLF angular velocities tracked the desired angular velocity with a small error, proving the CLF technique converges to the desired result. However, errors peaks observed in the EPW movement transitions require about 0.4 to $0.8\,s$ for stabilization in an about null error (below 0.2%). In addition, applying disturbances to the system, when the electrical voltage applied to the gearmotor is less than the electrical voltage supplied by the batteries (24 V), the CLF technique produce a greater control effort, in other words, there is a greater consumption of electrical voltage of the batteries, in order to compensate for this disturbance, seeking to keep the tracking of the angular velocity with a low error value. Whereas, due to open-loop control does not control the output signal of the system, this type of control becomes sensitive to the application of disturbances, causing the angular velocity tracking error to be proportional to the amplitude and the time of application of the disturbance.

Thus, moving the EPW, without the application of disturbances, the angular velocity tracking of the open-loop control and CLF techniques, even in the movements transition, is satisfactory and presents a small difference in the stabilization time in a about null error. Whereas, when applying disturbances in the system, the CLF presents a greater level of robustness than the open-loop control, in other words, the CLF technique presents a lower sensitivity to the disturbance, which minimizes the tracking error, when compared to open-loop control.

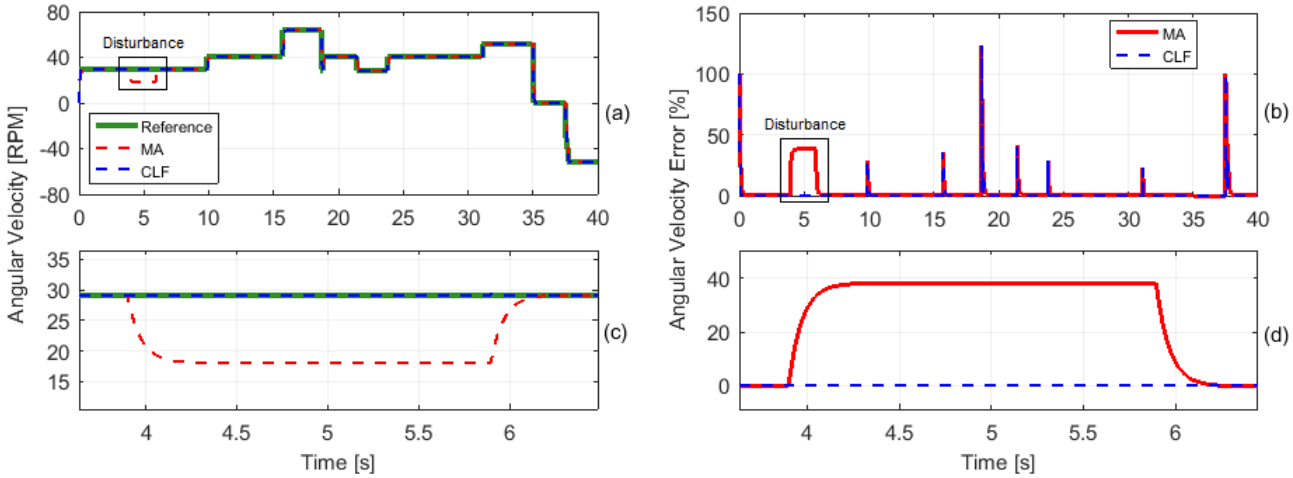

Figure 4. Left drive wheel - (a) Desired, Open-loop (MA) and CLF Angular Velocities vs. Time graph. (b) Error between Angular Velocities vs. Time graph. (c) Zoom in on specific point of the graph (a) (Disturbance). (d) Zoom in on specific point of the graph (b) (Disturbance).

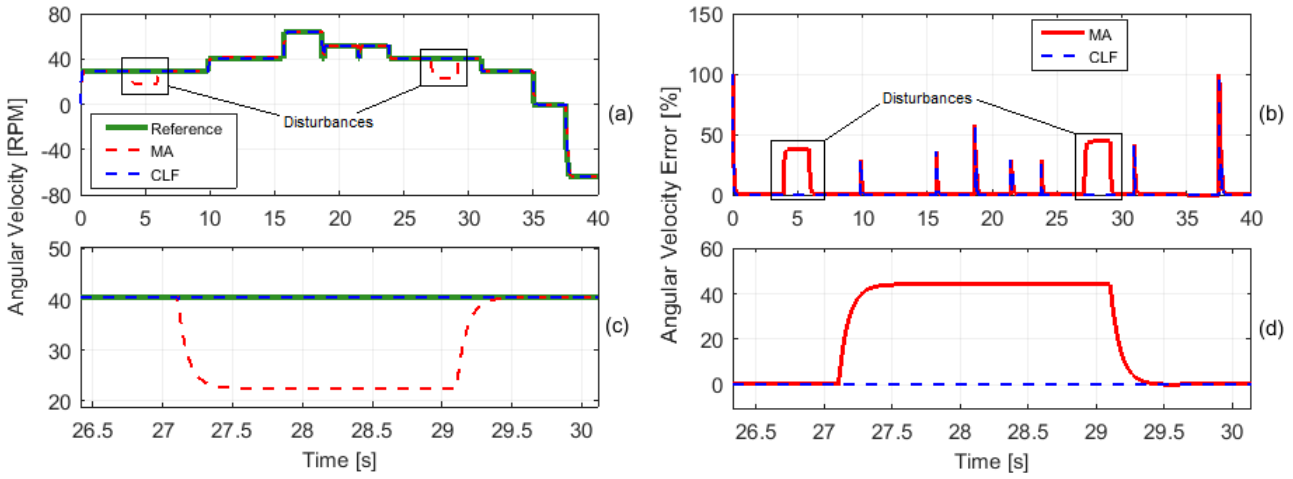

Figure 5. Right drive wheel - (a) Desired, Open-loop (MA) and CLF Angular Velocities vs. Time graph. (b) Error between Angular Velocities vs. Time graph. (c) Zoom in on specific point of the graph (a) (Disturbance). (d) Zoom in on specific point of the graph (b) (Disturbance).

Figure 6 shows the EPW position and orientation graphs (a) on a xy-plane and (b) on a xyz-space in a larger scale. The mathematical model proposed to the EPW has built a ramp at about 4° of slope as demonstrated as following.

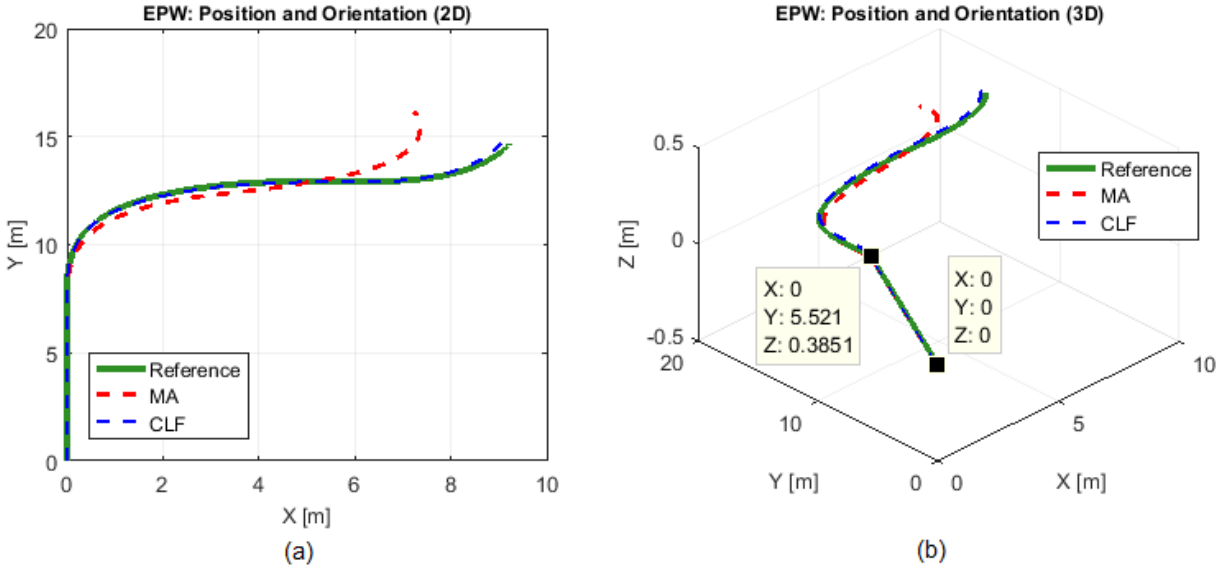

Figure 6. Position and orientation graphs of the EPW (a) on a 2D plane and (b) 3D space.

From Figure 6 (a), a considarable position error for the open-loop (MA) control can be verified, since the open-loop control is sensitive to the application of disturbances.

From the values given in the graph of Figure 6 (b), the slope angle of the ground can be calculated:

$$\phi_{Reference} = tan^{-1}\left(\frac{0.3851}{5.521}\right) \cong 3,99\,^{\circ} \cong 4\,^{\circ}\ .$$

A small difference was found in the value calculated for the slope angle of the ground (ramp), being justified due to the accounting for rounding errors that are generated during the numerical simulation.

4. CONCLUSION

This paper proposed the control Lyapunov function technique to control two drive wheels of an EPW, using the safe driving modelling, which controls the torque of the gearmotors. From the kinematic equations of an EPW that can moves on a flat and inclined surface, the dynamic equations were found, by using the Lagrangian formalism. Then, from the propulsion and rotation velocities, a mathematical model for controlling the EPW was proposed. Thus, from the mathematical model of the EPW, a graphical user interface was developed in MATLAB®/Simulink to intermediate the numerical simulations.

Through the numerical simulations, in situations without the application of disturbances, the angular velocities tracking of the open-loop control and CLF techniques, even in the movements transition, is satisfactory and presents a small difference in the stabilization time in a about null error. On the other hand, when applying disturbances in the system, the CLF presents a greater level of robustness than the open-loop control, in other words, the CLF technique presents a better performance.

Therefore, the mathematical model proposed for an EPW and the control law found for the CLF technique presented consistent and satisfactory results.

5. ACKNOWLEDGMENTS

The authors would like to thank CAPES for the financial support.

6. REFERENCES

Bloch, A.M., Baillieul, J., Crouch, P. and Marsden, J., 2003. *Nonholonomic Mechanics and Control*, Vol. 24. Springer, New York, USA.

Chua, J.J., Fuss, F.K. and Subic, A., 2010. "Rolling friction of a rugby wheelchair". *Conference of the International Sports Engineering Association (ISEA)*, Vol. 2, pp. 3071–3076.

Coelho, P.M.M., 2001. "Aplicação de lagrangianos na dinâmica de robôs móveis com rodas". *Technical report n^{o}ISR-LCIR-2001/01*.

Coelho, P.M.M. and Urbano, U.J.C., 2003. "Dinâmica de robôs móveis: Cadeira de rodas robotizada". *Ingenium, 2ª Série*, Vol. 77, pp. 70–73.

Cooper, R.A., 1999. "Engineering manual and electric powered wheelchairs". *Critical Reviews in Biomedical Engineering*, Vol. 27, pp. 27–73.

Fuss, F.K., 2009. "Influence of mass on the speed of wheelchair racing". *International Sports Engineering Association, springer*, Vol. 12, pp. 41–53.

Geiselhart, R., Gielen, R.H., Lazar, M. and Wirth, F.R., 2002. "Converse lyapunov theorems for discrete time systems: an alternative approach". *21st International Symposium on Mathematical Theory of Networks and Systems*, pp. 1298–1304.

Khalil, H.K., 2002. *Nonlinear Systems*. Prentice Hall, New Jersey, USA, 3rd edition.

Onyango, S.O., Hamam, Y., Djouani, K. and Daachi, B., 2016. "Modeling a powered wheelchair with slipping and gravitational disturbances on inclined and non-inclined surfaces". *Simulation: Transactions of the Society for Modeling and Simulation International –SAGE Journals*, Vol. 42(4), pp. 337–355.

Onyango, S.O., Hamam, Y., Djouani, K. and Qi, G., 2009. "Dynamic control of powered wheelchair with slip on an incline". *2nd International Conference on Adaptive Science & Technology*, pp. 278–283.

Park, J., Im, W., Kim, D. and Kim, J., 2014. "Safe driving algorithm of the electric wheelchair with model following control". *Published in Power Electronics and Applications. European Conference*, p. 10.

Riascos, L.A.M., 2015. "A low cost stair climbing wheelchair". *Published in IEEE 24th International Symposium on Industrial Electronics (ISIE)*, Vol. 1, pp. 627–632.

Siegwart, R. and Nourbakhsh, I.R., 2004. *Introduction to Autonomous Mobile Robots*. Bradford book, Massachusetts, USA.

Sontag, E.D., 1990. *Mathematical Control Theory: Deterministic Finite Dimensional Systems*. Springer, New York, USA.

Toudjeu, I.T., Hamam, Y., Karim, D., Wyk, B.J. and Monacelli, E., 2012. "Modelling and simulation of an user-wheelchair-envoiroment system". *Published in International Conference Modelling and Simulation*, pp. 198–204.

Ummat, S. and Kirby, R.L., 1994. "Nonfatal wheelchair-related accidents reported to the national electronic injury surveillance system". *American Journal of Physical Medicine and Rehabilation*, Vol. 73, pp. 163–167.

World Health Organization, 2011. "Summary - World Report on Desability". 13 Feb. 2017 <http://apps.who.int/iris/bitstream/10665/70670/1/WHO_NMH_VIP_11.01_eng.pdf>.

7. RESPONSIBILITY NOTICE

The authors are the only responsible for the printed material included in this paper.